A Security Measure for Signal Alignment based Packet Scheduling in Underwater Acoustic Communications

Yun Ye
City University of New York
New York, USA
yye@lagcc.cuny.edu

***Abstract*—This paper proposes a quantitative security measure for packet scheduling in underwater acoustic communications without data encryption. The transmitted data is protected through signal alignment by source nodes during packet scheduling in a way that the legitimate receiver is able to receive packets from all source nodes, while these packets collide with each other in a large portion of the remaining underwater areas. The underwater areas without packet collision are considered threatening when an attacker is present attempting to eavesdrop. Thus the volume of this threatening area is used as a metric to evaluate the security level of data communication adopting signal alignment based packet scheduling. In this work, the relation between the volume of the collision-free underwater area and the two essential parameters in packet scheduling, i.e. packet length and transmission delay, is explicitly formulated; and the procedure to control the volume of threatening area by tuning these two parameters, is explained.**

***Index Terms*—packet scheduling, signal alignment, underwater wireless network**

I. Introduction

Underwater wireless network (UWN) as a promising method to enhance human's capability of exploring the aquatic environment has attracted increasing attentions from both the academia and industry [1]–[5]. Different from terrestrial wireless communication with electromagnetic signals traveling in open air, in underwater environment especially seawater, acoustic signals are preferable in order to achieve long distance data transmission, since electromagnetic signals experience greater attenuation due to water's electrical conductivity and high permittivity.

A challenge of operating UWN is to secure transmitted information carried by acoustic waves. Existing systems broadcasting the requested information without any protection mechanism enable malicious users to eavesdrop on ongoing communications [6], [7]. In the literature, encryption based cryptography methods and signal alignment based methods without explicit encryption have been studied. For some UWNs, conventional cryptography methods including CDMA (code-division multiple access) cannot be applied directly as it involves key distribution, and it is computationally expensive [8], [9]. Instead the methods adopting signal alignment based packet scheduling among cooperative senders exploit low speed of acoustic waves to protect the data transmission process [3]–[5], [10], [11].

The principle of signal alignment based packet scheduling is to employ another sender (or more) in UWN as a cooperative helper sending additional signals modulated in the same frequency and transmitted with different delays to induce interference at unintended receivers, which is also known as jamming [12]. These schemes take advantage of long acoustic signal propagation delay in UWNs, and schedule the packet transmission in a way that the legitimate receiver is able to receive all the requested packets correctly, while these packets overlap or collide with each other at other areas. Since packet collision is time-space dependent, the packet scheduling is designed according to the distance between the senders and the legitimate receivers. For example, Zeng et al. propose an interference alignment algorithm in which each sender transmits payload in a dedicated time slot based on the estimated acoustic propagation delay at the receivers [10]. The packet transmission delay is calculated such that the intended receiver receives the message from a designated sender in a clear time window, and messages from other senders are corrupted due to their overlapping arrival time. Wang et al. describe another application scenario where packet delay and transmission power are jointly considered for multiple senders, in order to minimize the SINR (signal-to-interference-and-noise ratio) at the attacker under the SNR constraint of the legitimate receiver [3]. Casari et al. approach physical layer security through measuring channel features including relative root mean-square packet delay among sensor nodes in UWN to detect attackers [5].

In the study of these signal alignment based security strategies, quantitative formulation on the security level resulting from a specific packet delay scheduling scheme has not been included. In previous work, analysis on the geometry relation between the distribution of collision-free areas and the locations of the senders and receivers is provided in [11]. It is necessary to further specify the actual volume of the threatening area without packet collision susceptible to eavesdropping, in order to measure the security level of the selected packet scheduling scheme. And this volume information could serve as a reference for optimal system configuration on communication parameters under resource constraints [3], [4].

Based on these considerations, this work details the impact of packet scheduling with different configuration on the shape

and volume of resulting collision-free areas in the three-dimensional underwater space of interest. The scenario of one receiver with two cooperative senders is studied as theoretical foundation for analyzing more complex network structures. Two major parameters in packet scheduling that are related to the time-space effect of packet collision, namely packet length and transmission delay, and other constraints including propagation speed, transmission data rate and transmission power/range are used as parameters to construct the explicit formulation on the geometry shape and volume of threatening areas. The optimal configuration resulting in minimized volume of threatening areas is discussed accordingly.

The rest of the paper is organized as follows. Section II describes the mechanism of signal alignment based packet scheduling, the formulation on the relation between the shape and volume of threatening underwater areas and the packet scheduling parameters is derived in Section III, optimal configuration on packet scheduling parameters is described in Section IV, Section V discusses practical implementation, and conclusions are included in Section VI.

II. Signal Alignment based Packet Scheduling

Signal alignment based packet scheduling results in two different types of region in the three-dimensional underwater channel: the areas where packet collision occurs, and the areas where packets can be received without overlapping arrivals.

A. Packet Collision

Packet collision is caused by two packets not separated upon arrival at one location. To describe the geometry relation between the distribution of collision-free threatening areas and the locations of the senders and receiver, let s denotes the receiver location, $p = (x, y, z) \in \mathbb{R}^3$ denotes the sender location, $h(p, s) \in \mathbb{R}$ denotes the channel response from the sender to the receiver in a one hop communication scenario [13], and Y denotes the received signal from source signal U by the sender:

$$Y(s,t) = h(p,s)U(t-t) + N \tag{1}$$

N represents the additive channel noise. t is the end-to-end delay, including transmission delay t_h and propagation delay $\frac{d(p,s)}{c}$:

$$t = t_h + \frac{d(p,s)}{c} \tag{2}$$

$d(p, s)$ is the distance between the sender at p and the receiver s. c denotes the underwater acoustic signal propagation speed. It is considered invariant within the one hop communication.

At a receiver's location, two packets overlap with each other when one packet from j-th sender arrives in between the time duration when another packet from i-th sender is being received:

$$t_i - t_{p_j} < t_j < t_i + t_{p_i}, \quad i, j \in \mathbb{N} \tag{3}$$

$$t_{p_j} = \frac{l_j}{v} \tag{4}$$

$$t_j = t_{h_j} + \frac{d(p_j,s)}{c} \tag{5}$$

t_{p_j} is the transmission time related to the packet length l_j and data rate v. t_{h_j} is the transmission delay in packet scheduling for the j-th sender, and it is determined by Eqs. 3-5 to induce collision at the receiver.

Depending on whether the receiver is closer to the i-th sender, or is closer to the j-th sender, packet length and transmission delay scheduled for the j-th sender result in different distributions of areas with and without collision.

1) Receiver closer to the i-th sender:
Based on Eqs. 3-5, when the targeted collision spot s is closer to the cooperative sender at p_i, i.e. $d(p_i, s) < d(p_j, s)$, the transmission delay t_{h_j} for the sender at p_j, relative to the transmission time of the i-th sender ($t_{h_i} = 0$), can be scheduled according to Eq. 3:

$$\begin{aligned} -\frac{l_j}{v} - \frac{d(p_j,s) - d(p_i,s)}{c} < t_{h_j} \\ < \frac{l_i}{v} - \frac{d(p_j,s) - d(p_i,s)}{c} < \frac{l_i}{v} \end{aligned} \tag{6}$$

If t_{h_j} is set to the difference in propagation delays of the two paths $-\frac{d(p_j,s)-d(p_i,s)}{c}$, the two packets will arrive at s at the same time. t_{h_j} will be negative in this case.

$$\begin{aligned} &t_{h_j} = -\frac{d(p_j,s) - d(p_i,s)}{c}, \ \textit{or} \ \ \textit{equivalently} \\ &d(p_j,s) - d(p_i,s) = -t_{h_j} c \end{aligned} \tag{7}$$

In 3D geometry, all locations with constant distance difference to two foci form a circular hyperboloid surface. In this case, the two sender locations are the foci, and the receiver locations with identical packet arrival time represent the surface on the side of the i-th sender. Denote such a surface b_0 on which every spot including s has an identical difference $-t_{h_j} c$ in the distances to p_i and p_j:

$$b_0 = \{x | d(p_j, x) - d(p_i, x) = -t_{h_j} c, \ x \in \mathbb{R}^3\} \tag{8}$$

When two packets from two senders arrive at the same time, all spots on b_0, experience packet collision of the same signal alignment pattern. The geometry property described in Eq. 8 indicates that b_0 is a surface obtained by rotating one side of a hyperbola around its major axis crossing p_i and p_j. The intersection of b_0 with the plane containing s, p_i, p_j is displayed in Fig. 1a.

Eq. 6 defines two boundaries of the areas where packet collision occurs. These areas consist of the quadratic surfaces that contain spots of equal distance difference to the two senders. Consequently the two bounding surfaces are described as follows:

$$b_1 = \{x | d(p_j, x) - d(p_i, x) = \frac{l_i c}{v} - t_{h_j} c, \ x \in \mathbb{R}^3\} \tag{9}$$

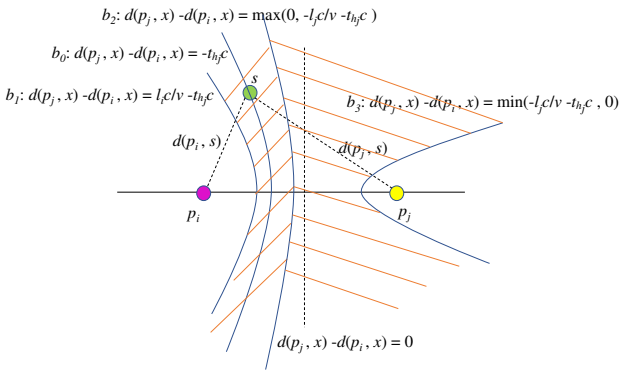

(a)

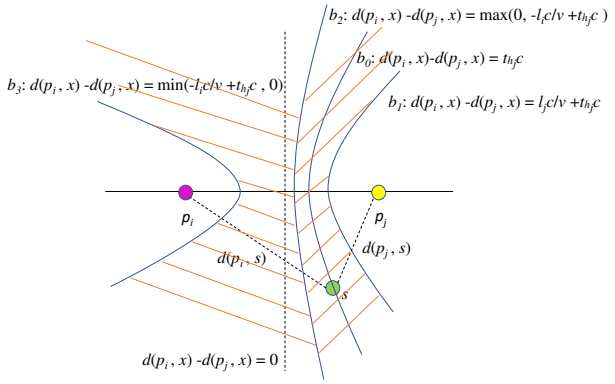

(b)

Fig. 1: Packet collision in shaded areas, (a) when the receiver is closer to the i-th sender, and (b) when the receiver is closer to the j-th sender.

$$
\begin{aligned}
b_2 =& \{x | d(p_j, x) - d(p_i, x) = \max(0, -\frac{l_j c}{v} - t_{h_j} c), \\
& x \in \mathbb{R}^3\}, \quad \textit{or equivalently} \\
b_2 =& \{x | d(p_j, x) - d(p_i, x) = -\frac{l_j c}{v} - t_{h_j} c, \\
& t_{h_j} \leq -\frac{l_j}{v}, \ x \in \mathbb{R}^3\}
\end{aligned} \tag{10}
$$

b_1 and b_2 each is formed by rotating one side of a distinctive hyperbola around the major axis crossing p_i and p_j. When $-\frac{l_j}{v} - t_{h_j} < 0$, b_2 extends to the other half of the underwater space divided by the plane perpendicular to and intersecting the line segment $\overline{p_i p_j}$ at its center, as shown in Fig. 1a. This bounding surface is a different quadratic surface facing the opposite direction, and it can be described as:

$$
\begin{aligned}
b_3 =& \{x | d(p_j, x) - d(p_i, x) = \min(-\frac{l_j c}{v} - t_{h_j} c, \ 0), \\
& x \in \mathbb{R}^3\}, \quad \textit{or equivalently} \\
b_3 =& \{x | d(p_j, x) - d(p_i, x) = -\frac{l_j c}{v} - t_{h_j} c, \\
& t_{h_j} \geq -\frac{l_j}{v}, \ x \in \mathbb{R}^3\}
\end{aligned} \tag{11}
$$

As will be discussed in Sec. IV, this observation on bounding surfaces provides inference for selecting packet length and transmission delay, in order to maximize the volume of the areas with packet collision, or equivalently, to minimize the volume of collision-free areas.

2) Receiver closer to the j-th sender: Similar to previous analysis, Fig. 1b demonstrates another scenario when the targeted collision spot s is closer to the sender at p_j, i.e. $d(p_i, s) > d(p_j, s)$, the transmission delay t_{h_j} for the sender at p_j, relative to the transmission time of the i-th sender ($t_{h_i} = 0$), can be scheduled according to the following constraint:

$$
\begin{aligned}
-\frac{l_j}{v} < -\frac{l_j}{v} + \frac{d(p_i, s) - d(p_j, s)}{c} < t_{h_j} \\
< \frac{l_i}{v} + \frac{d(p_i, s) - d(p_j, s)}{c}
\end{aligned} \tag{12}
$$

B. Packet Reception

The rest of the areas in the three-dimensional underwater space are collision free where the two packets are separated in time domain upon arrival. When the distance to the attacker is known to the senders, the transmission delay is selected according to Eq. 6 or 12 so that packet collision is induced. If the legitimate receiver is located or can be moved inside the collision-free areas, two packets are separable. If the legitimate receiver cannot be included in the collision-free areas, e.g. it resides on the same quadratic surface b_0 with the attacker, transmission power at the senders can be adjusted so that the signal strength is discernible between two overlapping packets [14].

In the more general case when the attacker's distance is unavailable to the senders, those collision-free areas (unshaded areas in Fig. 1) are considered threatening as long as the reception spot is within the communication range. For security consideration, the goal of the packet scheduling is to minimize the volume of these threatening areas. It can be achieved through formulating the numerical relation between this volume and related communication parameters. In other words, this volume is used as a metric to evaluate the security level of data communication in the three-dimensional underwater space of interest.

III. Formulation

For two packets to be separable at the legitimate receiver at r, the transmission delay t_{h_j} for the sender at p_j, relative to the transmission time of the other sender at p_i, is confined to the condition $t_{h_j} \geq \frac{l_i}{v} - \frac{d(p_j, r) - d(p_i, r)}{c}$ or $t_{h_j} \leq -\frac{l_j}{v} - \frac{d(p_j, r) - d(p_i, r)}{c}$, i.e. r is included in the non-shaded underwater areas bounded by b_1, b_2 or b_3 as shown in Fig. 1. Denote the threatening areas bounded by b_1 as I_1, the threatening areas bounded by b_2 as I_2, and the threatening areas bounded by b_3 as I_3:

$$
I_1 = \{x | d(p_j, x) - d(p_i, x) \geq \frac{l_i c}{v} - t_{h_j} c, \ x \in \mathbb{R}^3\} \tag{13}
$$

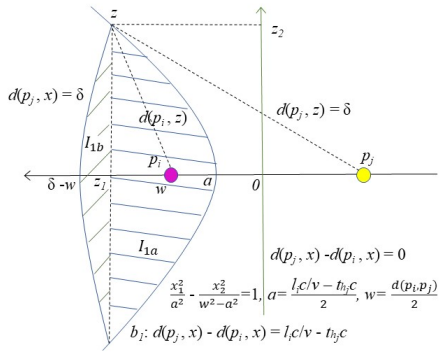

Fig. 2: Volume of threatening areas bounded by b_1 and f.

$$I_2 = \{x | d(p_j, x) - d(p_i, x) \leq -\frac{l_j c}{v} - t_{h_j} c, \; t_{h_j} \leq -\frac{l_j}{v}, \; x \in \mathbb{R}^3\} \tag{14}$$

$$I_3 = \{x | d(p_j, x) - d(p_i, x) \leq -\frac{l_j c}{v} - t_{h_j} c, \; t_{h_j} \geq -\frac{l_j}{v}, \; x \in \mathbb{R}^3\} \tag{15}$$

To estimate the volume of these areas, the geometry properties of the bounding surfaces displayed in Fig. 1 is utilized in the integral. For example, the intersection of b_1 with the plane containing s, p_i, p_j is one side of a hyperbola defined by

$$\frac{x_1^2}{a_1^2} - \frac{x_2^2}{w^2 - a_1^2} = 1, \; where \; a_1 = \frac{\frac{l_i c}{v} - t_{h_j} c}{2}, \; w = \frac{d(p_i, p_j)}{2}, \; 0 < a_1 < w, \; (x_1, x_2) \in \mathbb{R}^2 \tag{16}$$

The constant difference of distances between a point $x \in b_1$ and the two foci p_i and p_j, $d(p_j, x) - d(p_i, x)$, is the major axis of the hyperbola $2a_1$, as shown in Fig. 2. Assume the legitimate receiver requests data from the sender at p_j, given the communication range δ (longest distance for signal reception from sender at p_j), the threatening areas is also bounded by another spherical surface f with equal distance δ to p_j:

$$f = \{x | d(p_j, x) = \delta, \; x \in \mathbb{R}^3\} \tag{17}$$

As displayed in Fig. 2, the threatening areas are bounded by two surfaces b_1 and f, and the volume can be calculated with two separate integration:

$$V_{I_1} = V_{I_{1a}} + V_{I_{1b}} = \iiint_{I_{1a}} dx + \iiint_{I_{1b}} dx, \; x \in \mathbb{R}^3 \tag{18}$$

The two areas with volumes $V_{I_{1a}}$ and $V_{I_{1b}}$ are formed by rotating the two bounding curves represented by Eqs. 16 and 17. Therefore their volumes could be obtained through integration along the major axis. Since I_{1a} and I_{1b} intersect at a point $z = (z_1, z_2)$, Eqs. 16 and 17 are used to identify z_1, z_2:

$$z_1 = \frac{a_1 \delta - a_1^2}{w}, \; z_2 = \sqrt{\frac{(w^2 - a_1^2)(z_1^2 - a_1^2)}{a_1^2}} \tag{19}$$

Accordingly the volumes of I_{1a} and I_{1b} are obtained through integration

$$V_{I_{1a}} = \int_{a_1}^{z_1} \frac{\pi (w^2 - a_1^2)(u^2 - a_1^2)}{a_1^2} \, du, \; u \in \mathbb{R} \tag{20}$$

$$V_{I_{1b}} = \int_{z_1}^{\delta - w} \pi \left(\delta^2 - (u + w)^2\right) du, \; u \in \mathbb{R} \tag{21}$$

When $\delta \gg w$, $V_{I_{1b}}$ is negligible compared with $V_{I_{1a}}$, resulting in

$$V_{I_1} \approx V_{I_{1a}} = \pi a_1 (w^2 - a_1^2) \left(\frac{(\delta - a_1)^3}{3w^3} - \frac{\delta - a_1}{w} + \frac{2}{3} \right) \tag{22}$$

The volumes of I_2 or I_3 are obtained in a similar way:

$$V_{I_2} \approx V_I - \pi a_2 (w^2 - a_2^2) \left(\frac{(\delta - a_2)^3}{3w^3} - \frac{\delta - a_2}{w} + \frac{2}{3} \right) \tag{23}$$

$$V_{I_3} \approx \pi a_3 (w^2 - a_3^2) \left(\frac{(\delta + a_3)^3}{3w^3} - \frac{\delta + a_3}{w} + \frac{2}{3} \right) \tag{24}$$

$$V_I = \frac{4}{3} \pi \delta^3 \tag{25}$$

V_I is the volume of the underwater areas within the communication range of the sender at p_j. a_2 and a_3 are the semi major axes of two hyperbolas with the same linear eccentricity w described in Eq. 16:

$$a_2 = \frac{\frac{-l_j c}{v} - t_{h_j} c}{2} \tag{26}$$

$$a_3 = \frac{\frac{l_j c}{v} + t_{h_j} c}{2} \tag{27}$$

Adding the volumes of the two unshaded areas shown in Fig. 1, the total volume of the threatening areas is expressed as

$$V = \begin{cases} V_{I_1} + V_{I_2}, & \text{if } t_{h_j} < -\frac{l_j}{v}; \\ V_{I_1} + V_{I_3}, & \text{otherwise} \end{cases} \tag{28}$$

With proper selection of packet length and transmission delay, this volume can be minimized to protect data communication to the maximum extent.

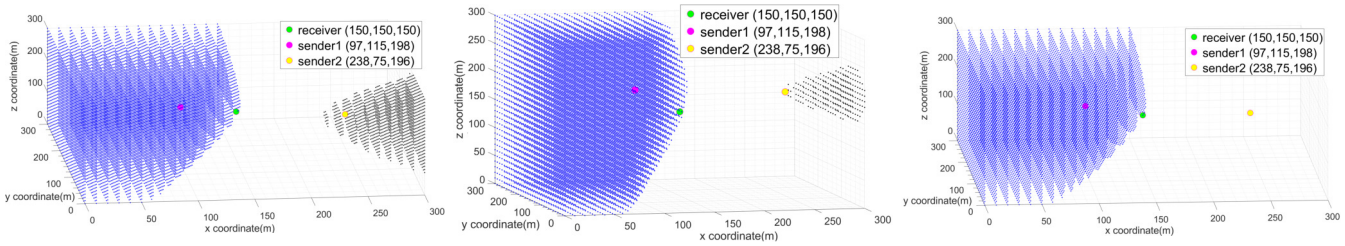

Fig. 3: Threatening areas in a $(0, 300) \times (0, 300) \times (0, 300)$ underwater space. From left to right, the packet length for the two senders is set to 300 bits, 500 bits and 700 bits, respectively. $r = (150, 150, 150),\ p_i = (97, 115, 198),\ p_j = (238, 75, 196),\ c = 1.5\ km/s,\ v = 10\ kbps.$

IV. Optimal Parameter Selection

From previous analysis on geometry distribution of the threatening areas, V_{I_1} is minimized when t_{h_j} is chosen to have the legitimate receiver locate on b_1 ($r \in b_1$) provided the condition that two packets are separable at the legitimate receiver:

$$t_{h_j} = \frac{l_i}{v} - \frac{d(p_j, r) - d(p_i, r)}{c} \tag{29}$$

Meanwhile, to minimize the threatening areas on the other side, i.e. V_{I_3} ($t_{h_j} \geq -\frac{l_j}{v}$ is preferred due to $V_{I_2} \geq V_{I_3}$), since $r \notin I_3$, the strategy is to turn V_{I_3} to zero through setting the semi major axis no less than the linear eccentricity:

$$\begin{aligned} &a_3 \geq w,\ \textit{or equivalently} \\ l_j \geq \frac{d(p_i, p_j)v}{c} &+ \frac{(d(p_j, r) - d(p_i, r))v}{c} - l_i \end{aligned} \tag{30}$$

Once the packet length of the cooperative helper at p_i is known, the optimal configuration of packet length and relative transmission delay for the sender at p_j is determined according to Eq. 29 and 30. Fig.3 demonstrates the distribution of collision-free threatening areas resulted from different packet lengths in MATLAB simulation. The 300 m $\times$ 300 m $\times$ 300 m underwater area is sampled at 10 m intervals. The legitimate receiver represented by the green dot is placed at the center. The locations of the first sender represented by the magenta dot and the second sender represented by the yellow dot are randomly generated. Each location is examined for packet collision status using Eqs.13-15. The transmission delay for the second sender is calculated as $t_{h_2} = \frac{l}{10^4} - \frac{124.44 - 79.61}{1500}$ according to Eq. 29, so that minimum V_1 is achieved while the legitimate receiver is included at the surface of I_1. Locations in I_1 are displayed as the blue dot, and locations in I_3 are displayed as the black dot. When the packet length $l = 700$ bits, we have $t_{h_2} = 0.04\ s$, and subsequently, $a_3 = \frac{700 \times 1500/10^4 + 0.04 \times 1500}{2} = 82.5\ m$, $w = \frac{146.58}{2} = 73.29\ m$. The condition expressed in Eq. 30 is satisfied, i.e. the semi major axis a_3 is longer than the linear eccentricity w. Thus no hyperbola is formed to contain the threatening area I_3 ($V_{I_3} = 0$). This packet scheduling scheme is considered the securest among the three, in terms of minimum volume of threatening area which could be evaluated using Eq. 22. Note that further increasing packet length will not change this security measure.

V. Discussion

In underwater environment, the speed and trajectory of the acoustic signal varies depending on the depth, salinity, temperature of the location, and selection of the transmission delay can be adjusted according to the estimated propagation delay and statistical characterization of the channel [13]. In the presence of time synchronization and distance measurement distortion, transmission delay is modified to enlarge the volume of b_1, i.e. to have the legitimate receiver $r \in I_1, r \notin b_1$, so that there is redundancy for packet separation at the legitimate receiver. Another parameter, the transmission data rate v, can be considered to increase flexibility in packet scheduling.

When more helpers are employed, similar process of deriving the security measure to minimize the threatening areas can be applied. The resulting threatening areas are bounded by multiple hyperboloids, and the volume of the threatening areas will be further reduced.

VI. Conclusion

The security measure described in this work enables quantitative evaluation on signal alignment based data protection schemes in UWNs. In resource constrained UWNs, signal alignment based data protection is attractive when cryptography methods including CDMA based spectrum spreading are infeasible, and when the attacker distance is unknown. The explicit formulation on numerical relation between the volume of collision-free threatening underwater areas and the major packet scheduling parameters provides theoretical foundation for implementing signal alignment based secure communications in UWN.

References

[1] Mandar Chitre, Lee Freitag, Ethem Sozer, Shiraz Shahabudeen, Milica Stojanovic, and John Potter. An Architecture for Underwater Networks. In *Proc. IEEE OCEANS*, 2006.

[2] Keyu Chen, Maode Ma, En Cheng, Fei Yuan, and Wei Su. A Survey on MAC Protocols for Underwater Wireless Sensor Networks. *IEEE Communications Surveys and Tutorials*, 16(3):1433–1447, 2014.

[3] Chaofeng Wang and Zhaohui Wang. Signal alignment for secure underwater coordinated multipoint transmissions. *IEEE Transactions on Signal Processing*, 64(23):6360–6374, 2016.

[4] Zheng Peng, Xu Han, and Yun Ye. Enhancing underwater sensor network security with coordinated communications. In *IEEE International Conference on Communications*, pages 1–6, 2021.

[5] Paolo Casari, Roee Diamant, Stefano Tomasin, Jeff Neasham, Lutz Lampe, et al. Practical security for underwater acoustic networks: published results from the safe-ucomm project. In *Proc. of the 10th Convention of the European Acoustics Association*, pages 5685–5692, 2023.

[6] Alexander Afanasyev, Priya Mahadevan, Ilya Moiseenko, Ersin Uzun, and Lixia Zhang. Interest Flooding Attack and Countermeasures in Named Data Networking. In *2013 IFIP Networking Conference*, Brooklyn, NY, USA, 2013.

[7] Alberto Compagno, Mauro Conti, Paolo Gasti, and Gene Tsudik. Poseidon: Mitigating Interest Flooding DDoS Attacks in Named Data Networking. In *38th Annual IEEE Conference on Local Computer Networks*, Sydney, NSW, Australia, 2013.

[8] Huacheng Zeng, Y Thomas Hou, Yi Shi, Wenjing Lou, Sastry Kompella, and Scott Midkiff. Shark-ia: An interference alignment algorithm for multi-hop underwater acoustic networks with large propagation delays. 11 2014.

[9] Yu Luo, Lina Pu, Zheng Peng, and Zhijie Shi. RSS-Based Secret Key Generation in Underwater Acoustic Networks: Advantages, Challenges, and Performance Improvements. *IEEE Communications Magazine*, 54(2):32–38, 2016.

[10] Hovannes Kulhandjian, Tommaso Melodia, and Dimitrios Koutsonikolas. Securing underwater acoustic communications through analog network coding. In *2014 Eleventh Annual IEEE International Conference on Sensing, Communication, and Networking*, pages 266–274, June 2014.

[11] Yun Ye, Zheng Peng, Arun Raj Kumar P, Vasudevan A R, and Xiaoyan Hong. Active jamming for eavesdropping prevention in underwater wireless networks. Atlanta, GA, USA, 10 2019.

[12] Kanika Grover, Alvin Lim, and Qing Yang. Jamming and anti-jamming techniques in wireless networks: A survey. *Int. J. Ad Hoc Ubiquitous Comput.*, 17(4):197–215, December 2014.

[13] Milica Stojanovic and James Preisig. Underwater Acoustic Communication Channels: Propagation Models and Statistical Characterization. *IEEE Communications Magazine*, 47(1):84–89, 2009.

[14] Jianwei Xie and Sennur Ulukus. Secure degrees of freedom of one-hop wireless networks. *IEEE Transactions on Information Theory*, 60(6):3359–3378, 2014.